Assembly of Aptamer Switch Probes and Photosensitizer on Gold Nanorods for Targeted Photothermal and Photodynamic Cancer Therapy

Jian Wang,[†,‡] Guizhi Zhu,[†,§] Mingxu You,[†] Erqun Song,[†,‡] Mohammed Ibrahim Shukoor,[†] Kejing Zhang,[†] Meghan B. Altman,[†] Yan Chen,[†,§] Zhi Zhu,[†,§] Cheng Zhi Huang,[‡,*] and Weihong Tan[†,§,*]

[†]Department of Chemistry and Department of Physiology and Functional Genomics, Shands Cancer Center and Center for Research at the Interface of Bio/Nano, UF Genetics Institute and McKnight Brain Institute, University of Florida, Gainesville, Florida 32611-7200, United States, [‡]Education Ministry Key Laboratory on Luminescence and Real-Time Analysis, College of Pharmaceutical Science, College of Chemistry and Chemical Engineering, Southwest University, Chongqing 400715, People's Republic of China, and [§]Molecular Science and Biomedicine Laboratory, State Key Laboratory of Chemo/Bio-Sensing and Chemometrics, College of Biology and College of Chemistry and Chemical Engineering, Hunan University, Changsha, 410082, People's Republic of China

ABSTRACT

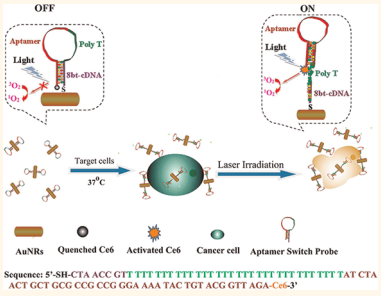

An aptamer switch probe (ASP) linking chlorin e6 (Ce6), a photosensitizer molecule, to the surface of gold nanorods (AuNRs) was used to target cancer cells for photodynamic therapy (PDT) and photothermal therapy (PTT). In the presence of target cancer cells, the ASP changes conformation to drive Ce6 away from the gold surface, thereby producing singlet oxygen for PDT upon light irradiation. Since each AuNR is modified with many ASP-Ce6 molecules, the AuNR-ASP-Ce6 conjugate yields enhanced binding and therapeutic effect by the added ability to carry many photosensitizers. In addition, absorption of radiation by the gold nanorods enables further cell destruction by the photothermal effect. Consequently, this multimodal AuNR-ASP-Ce6 conjugate offers a remarkably improved and synergistic therapeutic effect compared to PTT or PDT alone, providing high specificity and therapeutic efficiency, which can be generalized to other types of cancer therapies.

KEYWORDS: gold nanorods · photosensitizer · aptamer switch probe · cancer therapy

Multimodality is a new, but very promising, advancement in cancer diagnosis, therapy, and targeted molecular imaging,[1] because of the higher efficacy of combinational treatment and the simultaneous monitoring of therapeutic effects. In previous research, the photosensitizer/gold nanorod (AuNR) complex has been used as a combinational photodynamic therapy/photothermal therapy (PDT/PTT) strategy.[1−3] In these multimodalities, the photosensitizers used in PDT are usually nonphototoxic when they are nonfluorescent even under light illumination (an "off" state). However, when these sensitizers are active (an "on" state), they become actively phototoxic and generate reactive oxygen species (ROS) including singlet oxygen for PDT upon light illumination;[4,5] The AuNRs also serve as ultraefficient energy quenchers[1,3] and hyperthermia agents for PTT[6,7] as a consequence of their unique strong surface plasmon absorption band in the near-infrared (NIR) region. The above multimodalities supply higher oncolytic efficacy compared to use of either PDT or PTT alone. However, these previous approaches utilized photosensitizers that are electrostatically adsorbed onto the surface of AuNRs by a polymer layer, making it impossible to control the targeted release of singlet oxygen.[1,3] This lack of specificity has resulted in unavoidable damage to nontarget cells.[3]

Aptamer−nanomaterial conjugates can be used to achieve multimodality with molecular specificity.[8−10] Briefly, aptamers are single-stranded DNA or RNA (ssDNA or ssRNA) selected from pools of random-sequence oligonucleotides to bind a wide range of targets, including intact cells, with high affinities and specificities.[11−13] Compared to antibodies, aptamers offer significant advantages, such as flexible design, synthetic accessibility, easy modification, chemical stability, and rapid tissue penetration.[14] Aptamers have been widely applied

* Address correspondence to tan@chem.ufl.edu, chengzhi@swu.edu.cn.

Received for review February 15, 2012 and accepted May 25, 2012.

Published online May 25, 2012
10.1021/nn300694v

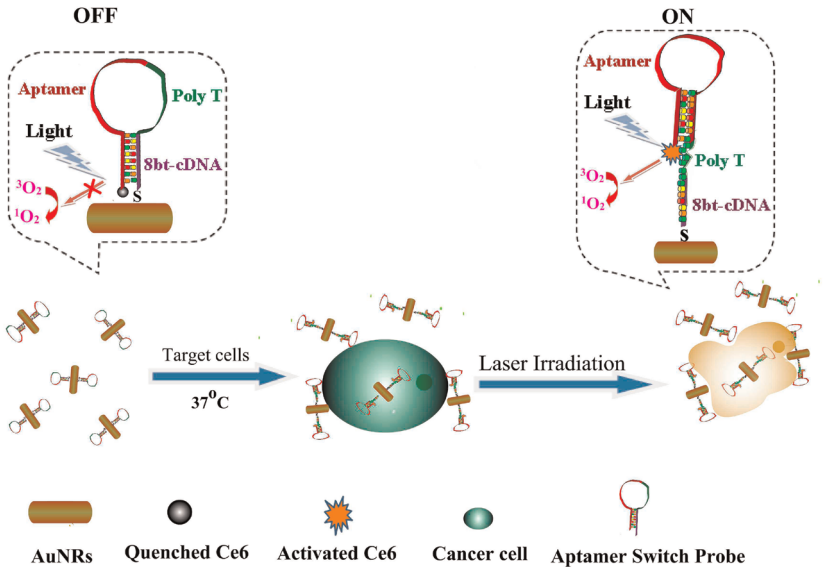

Sequence: 5'-SH-CTA ACC GTT TTT TTT TTT TTT TTT TTT TTT TTT TTT TAT CTA ACT GCT GCG CCG CCG GGA AAA TAC TGT ACG GTT AGA-Ce6-3'

Scheme 1. Schematic representation of ASP–photosensitizer–AuNRs for PTT and PDT.

in cancer recognition,[15,16] diagnosis,[17] drug delivery,[18–21] and therapy.[7,22–24] Aptamers have also been linked to AuNRs for targeted PTT[7] or modified with photosensitizers for specific PDT.[23]

In this work, a leukemia cell line was used as the target cancer cells to study the combinatorial PDT/PTT. Current clinical approaches for leukemia therapy primarily involve chemotherapy and bone marrow transplantation. However, these represent a rather narrow spectrum of therapeutic regimens compared to the number available for solid tumors. In solid tumors, cancer cells are highly concentrated, allowing therapeutic agents to accumulate at tumor sites through enhanced permeation and retention. In contrast, leukemia cells are widespread in the circulatory system and are surrounded by normal blood cells.[25] Under these circumstances, any nonspecific cytotoxin[26] would also destroy normal blood cells, thereby affecting the oxygen supply to the tissues and the entire immune system. Therefore, a targeted, robust therapy that could specifically kill leukemia cells, while leaving normal cells unharmed, would be highly desirable.

Using a combinatorial PDT/PTT approach in the present work, aptamer switch probe (ASP)-modified AuNRs were designed to carry chlorin e6-polyvinylpyrrolidone (Ce6-PVP)[27] to the target cancer cells. In this approach, PDT is controlled by singlet oxygen generation (SOG) achieved by manipulating the quenching and recovery of photosensitizer fluorescence, which is, in turn, tuned by controlling the distance between the quencher and photosensitizer. The cancer cells can be selectively destroyed by illumination with white light during PDT, while minimizing phototoxic tissue damage to the surrounding normal tissues. In this work, AuNRs served as photosensitizer carriers and quenchers to manipulate the targeted PDT, as well as hyperthermia agents to kill target cancer cells upon laser irradiation. Due to the synergistic effect, the therapeutic efficacy of AuNRs–photosensitizer complexes was enhanced compared to PDT or PTT alone.

RESULTS AND DISCUSSION

To achieve the targeted PDT, the fluorescence of the aptamer-conjugated photosensitizer should be quenched in the absence of target and be recovered when target is present. The sgc8 leukemia aptamer by itself is an "always-off" aptamer, which remains in its hairpin form when linked to a gold surface. If the aptamer remained in this state, the photosensitizer would always be quenched, leaving it nonphototoxic even under light illumination. If a polyethylene glycol (PEG) spacer was introduced to the 3′-end or 5′-end to activate the fluorescence, the PEG-linked sgc8 would become an "always-on" aptamer,[6] resulting in a high background. To control the quenching and recovery of fluorescence, an ASP was developed,[28,29] which also used an activatable aptamer probe to control the activity of the photosensitizer for targeted destruction.

Our strategy for multimodal therapy and the sequence of ASP are shown in Scheme 1. As presented, the photosensitizer Ce6 is connected to the 3′-end of ASP *via* the coupling between the carboxyl group of the Ce6 molecule (the chemical structure is presented in Figure S1) and the amino group at the 3′-end of sgc8, an aptamer for acute lymphoblastic leukemia T-cells. A poly-T chain links the 5′-end of sgc8 to an 8-base segment complementary to sgc8, which ends in a

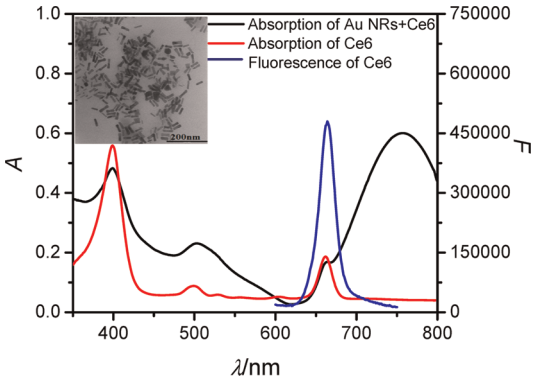

Figure 1. Absorption spectra of the AuNRs-Ce6 complex and free Ce6; emission spectrum of free Ce6. Inset: TEM image of AuNRs.

sulfhydryl group for attachment to AuNRs. Unlike the typical "always-on" aptamer probes, which are characterized by high backgrounds and limited contrast, the ASP, which is a molecular beacon aptamer, exhibits quenched fluorescence in its free "off" state, but undergoes a structural change upon binding to target cancer cells in its "on" state.[28] Thus, in the absence of target cancer cells, photosensitization by Ce6 is inhibited by proximity to the AuNR surface based on hybridization of the 8-base segment with part of sgc8 and overlap of the Ce6 emission and AuNR absorption bands.[3] However, when a target cancer cell is present, it binds to the aptamer, disrupting the hybridization to the 8-base segment. As a result, the sgc8 aptamer self-hybridizes to form its usual hairpin structure. The poly-T then extends out, allowing Ce6 to move away from the gold surface, effectively removing the quenching effect. Subsequent light irradiation causes singlet oxygen, $^1O_2$, to be released to destroy the cancer cells by PDT. In addition to being ultraefficient quenchers for photosensitizer Ce6, AuNRs can carry multiple Ce6-ASPs to induce a high local concentration of photosensitizer to kill the target cells more efficiently. Furthermore, photothermal agent AuNRs can convert laser light to heat,[30] which dissipates in the surrounding microenvironment to kill cancer cells. In this therapeutic mode, the combined singlet oxygen generation and heat energy lead to more effective cell destruction due to the synergistic effect.

Gold NRs with cetyltrimethylammonium bromide (CTAB) surfactant coating were synthesized following a seed-mediated protocol.[31] As displayed in Figure 1, the aspect ratio of the AuNRs was about 3.3, and the longitudinal plasmon resonance absorption (LPRA) band was located in the NIR region. To prevent aggregation of AuNRs during the conjugation process and reduce the toxicity of AuNRs, thiol-terminated poly(ethylene glycol) (mPEG-SH) was conjugated on the AuNR surfaces *via* thiol chemistry.[7]

The Ce6 used in this study is a second-generation photosensitizer with good optical properties and high quantum efficiency for singlet oxygen production,[5] which has been widely used for PDT.[5,23,32] In addition, the absorption peaks of Ce6 are at 397, 510, and 664 nm with emission at 664 nm, which overlaps the wide LPRA of AuNRs. Since the LPRA of AuNRs in the NIR region overlapped with the emission band of Ce6 (Figure 1), the fluorescence and SOG of Ce6 could be inhibited due to energy transfer from the excited Ce6 to AuNRs when Ce6 is close to the gold surface, thereby reducing the Ce6 background signal.

In the therapeutic work, it is important to target only particular cell types, thereby limiting side effects that result from nonspecific delivery. To check the specificity, aptamer sgc8, which binds the cell membrane protein tyrosine kinase-7 (PTK7) with high affinity and selectivity,[33] was used in our study with different types of cell lines, including target cancer cell CCRF-CEM (acute lymphoblastic leukemia T-cells) and negative control Ramos cells (acute lymphoblastic leukemia B-cells). For these experiments, the aptamer was labeled with a FAM fluorophore. The flow cytometry results in Figure 2 show that target CCRF-CEM cancer cells showed strong fluorescence signal at both 4 and 37 °C. However, the fluorescence signal of the control Ramos cells was as weak as that from cells only at either 4 or 37 °C. Moreover, a random library (Lib) sequence was used as a control sequence to study the specific binding. The data showed that for both target cancer cells and nontarget cells the Lib gave a signal as weak as that from cells only, suggesting that nonspecific binding or internalization of Lib was very slow under our conditions. Trypsin was used to remove the anti-PTK7 aptamer target on the cell membrane.[34] After trypsin treatment, the fluorescence signal from flow cytometry of CCRF-CEM was very weak at 4 °C, but it still showed a high fluorescence signal at 37 °C, which can be attributed to the binding of aptamer to the cell membrane protein at 4 °C and the internalization at 37 °C.[34] To achieve enhanced therapy, we incubated aptamer with cells at 37 °C for further study.

To monitor the sgc8 internalization dynamic process, the time and dose dependence of internalization were studied by flow cytometry. It was reported that due to the internalization function of PTK7, sgc8 was taken up by cells and delivered into the endosomes.[34] Therefore, the target cancer cells showed a higher internalization rate than nontarget ones. As shown in Figure 3, a much stronger signal was achieved with longer incubation time and higher concentrations for both CCRF-CEM and Ramos. That is, more aptamers can be carried into the cancer cells with higher aptamer concentration or longer incubation time within 1.5 h. It should be noted that nonspecific binding of aptamer and Ramos occurred when the incubation time was longer than 2 h. Therefore, the cells were incubated with probes for less than 2 h to reduce the nonspecific internalization.

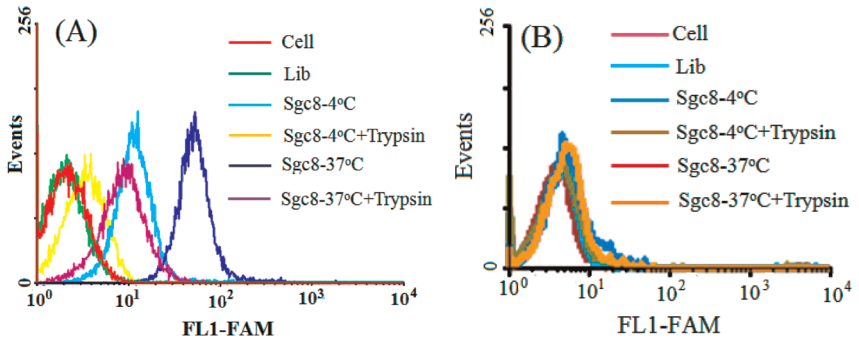

Figure 2. Flow cytometry results of aptamer binding with CCRF-CEM (A) and Ramos (B) under different conditions. (All flow data were recorded with FAM because there is no channel available to detect Ce6 in flow cytometry.) Cells, 200k/sample; sgc8, 200 nM.

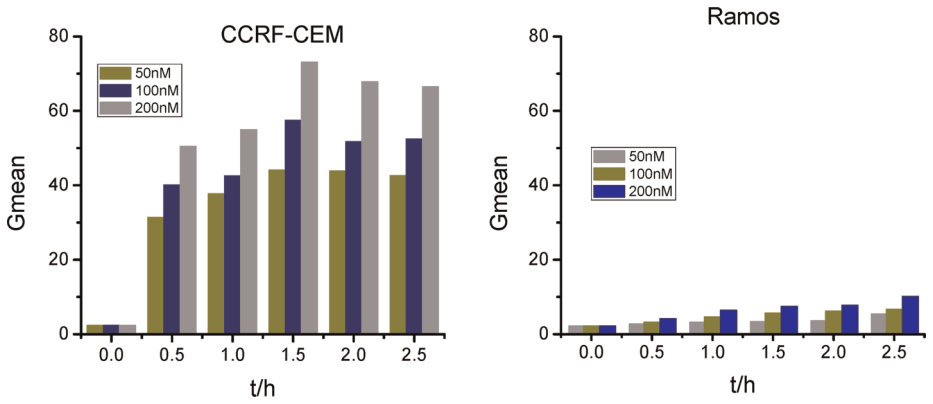

Figure 3. Time- and dose-dependent binding of sgc8 with cancer cells at 37 °C. Cells, 200k/sample; sgc8, 200 nM.

We also studied the specific binding of the ASP with CCRF-CEM and Ramos to determine the effect of the poly-T linker length in the ASP by flow cytometry. As shown in Figure 4, for the unconjugated ASP, the binding affinity increased with longer T linker, while for the ASP-NRs (Figure 4A), the binding affinity increased from 8 to 32 T bases, but dropped back at 40 T bases (Figure 4B). The enhancement in binding affinity with up to 32 T results from the increased distance between the fluorophore and the gold surface, leading to the recovery of fluorescence. The decrease above 32 T bases may have been caused by increased flexibility, which allows the fluorophore to move closer to the gold surface. The optimum 32 T spacer length was used for further experiments. In this case, the distance between gold surface and photosensitizer is 40bp, including 32 T bases and 8 complementary bases. It is noteworthy that the ASP-NRs showed a much stronger fluorescence signal in flow cytometry, which may be attributed to the attachment of multiple ASPs on each AuNR.[6,7] The control experiment was checked with Ramos cells (Figure 4C and D), which showed that both ASPs and ASP-AuNRs could induce only a weak nonspecific internalization, which suggests that nonspecific recognition internalization occurred at a very slow rate, leading to high specific internalization by the target cancer cells.

For targeted PDT, photosensitizer molecules Ce6 were linked to ASP-T_{32}-NR conjugates, and the SOG was determined with a singlet oxygen indicator: singlet oxygen sensor green (SOSG).[23,35] In 50% D_2O, the SOSG signal of Ce6-ASP-T_{32} was quenched when linked to the AuNR surface (Figure S2), but it was enhanced by 3.5 times by addition of the complementary DNA (cDNA) of ASP-T_{32} (Figure 5), which allowed Ce6 to move away from the gold surface to produce a strong SOSG signal. Compared with cDNA, CCRF-CEM cells showed a less enhanced SOSG signal, because the formation of dsDNA (81 bt) allows Ce6 to move farther from the AuNR than the binding to CCRF-CEM cells (40 bt). In addition, lack of spatial hindrance caused by cell binding allowed more cDNA to hybridize with Ce6-ASP-T_{32}, moving more Ce6 away from gold surface to produce singlet oxygen. There was no recovery of SOSG in the presence of Ramos cells, showing that SOG can be used for selective photodynamic treatment of CCRF-CEM cancer cells.

Cell destruction by both PDT and PTT was studied by irradiation with either white light or an 812 nm NIR laser. As indicated by the SOSG studies, singlet oxygen is produced after binding of CCRF-CEM. Therefore, as shown in Figure 6, the cell viability decreased with increasing light illumination. However, when the illumination period was longer than 3 h, the cell viabilities

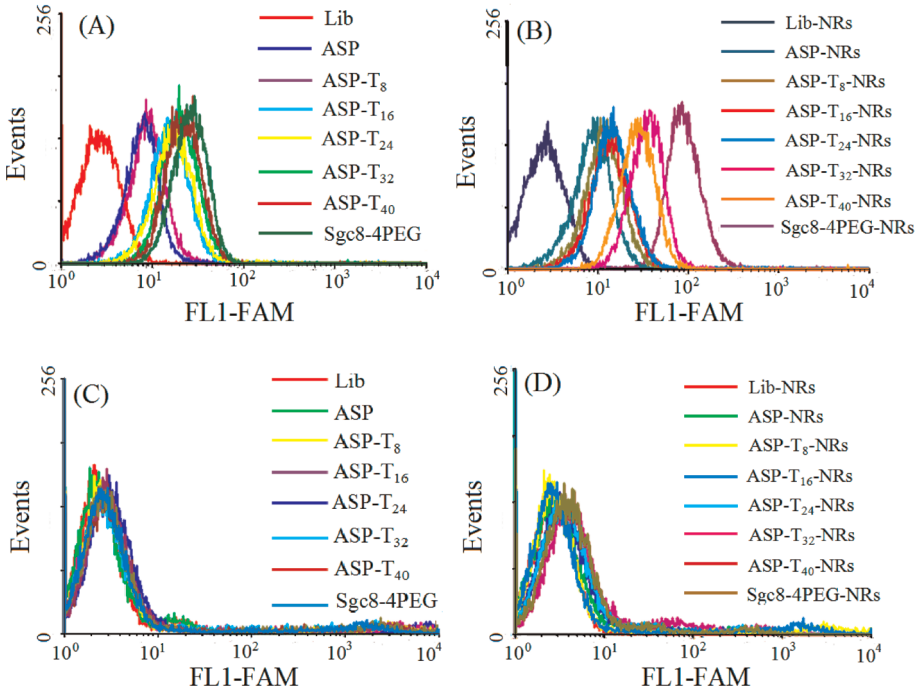

Figure 4. Cell binding of FAM-modified aptamer and aptamer–AuNRs conjugates with cells: (A, B) CCRF-CEM and (C, D) Ramos. Aptamers, 200 nM; aptamer–AuNRs, 0.2 nM; incubation time, 2 h.

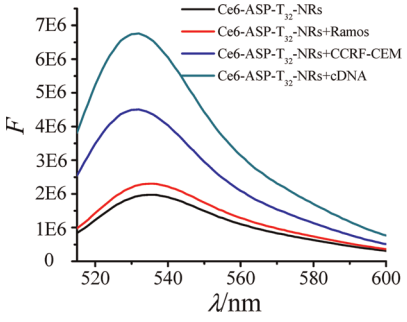

Figure 5. Fluorescence of SOSG for Ce6-labeled ASP-T_{32}-NR conjugates under different conditions. Concentrations: Ce6-ASP-T_{32}-NR, 0.2 nM; cDNA, 200 nM; cells, 200k/sample.

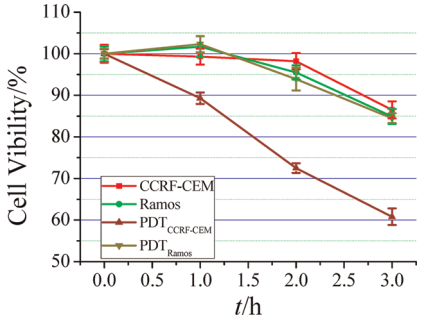

Figure 6. Photodynamic therapy under white light for different irradiation times. Cells, 200k/sample; probes, 0.2 nM.

of CCRF-CEM and Ramos were both lower than 90%. Therefore, a 2 h irradiation with white light was employed for PDT studies. White light showed only slight harm to cells without photosensitization. With target CCRF-CEM, the Ce6-ASP caused significant cell destruction under white light illumination, but the Ramos control cells showed high cell viability.

As thermal agents, AuNRs are able to convert light to heat for PTT.[6,36] During laser irradiation, the temperature of the solution increased from about 25 °C to 55 °C when ASP-NRs were incubated with CCRF-CEM (Figure 7A). However, in the absence of AuNRs, or if ASP-NRs were incubated with nontarget cancer cells, the temperature remained lower than 37 °C. After laser irradiation, cell death was determined using propidium iodide (PI) dye and monitored by flow cytometry, as shown in Figure 7B. The results indicate that CCRF-CEM with AuNRs-ASP-Ce6 showed a high PI signal, but cells without AuNRs, or AuNRs with nontarget Ramos cells, showed a weak PI signal, indicating that probe–target selectivity allows photothermal destruction of target cells. Furthermore, a synergistic effect was observed during the PTT (Figure S2 and S3). The fluorescence spectra were recorded before and immediately after NIR irradiation (Figure S2). Since the temperature of the solution without AuNRs did not increase appreciably (Figure 7), the fluorescence of Ce6-ASP-T_{32} changed very little. For Ce6-ASP-T_{32}-NR, the system could reach a higher temperature than the melting temperature of ASP-T_{32} (46.1 °C, calculated with Integrated DNA Technologies Oligo Analyzer software) and provide a higher percent of fluorescence enhancement. The NRs absorb the light of the NIR laser to produce heating to accelerate the change of the ASP structure, leading to the release of Ce6 from the gold surface,[37] resulting in enhanced PDT. Figure 3 shows the dynamic fluorescence signal of SOSG using a temperature controller to

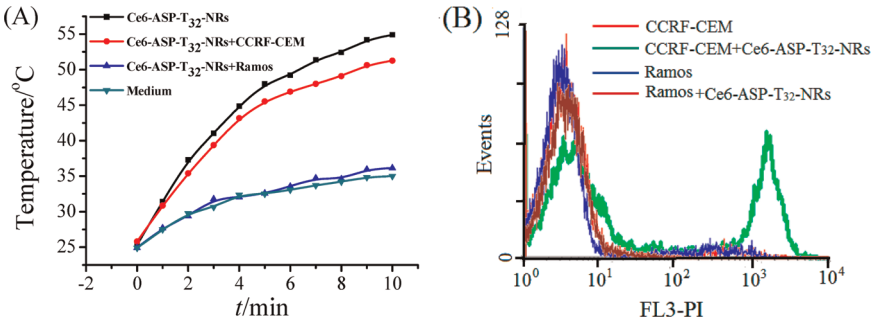

Figure 7. (A) Temperature−time curves of Ce6-labeled ASP-T_{32}-NR complex and (B) photothermal therapy results with laser irradiation. sgc8-NRs, 0.2 nM; cells, 200 k/sample; probes, 200 nM; laser wavelength, 812 nm.

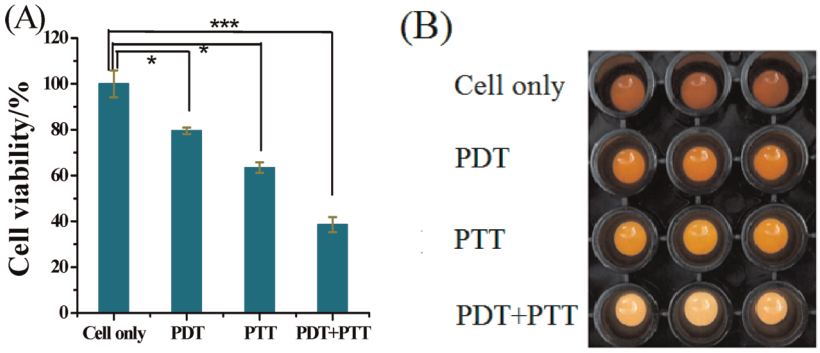

Figure 8. Cell viability data (A) and imaging (B) of CCRF-CEM cells incubated with Ce6-ASP-T_{32}-NRs without light irradiation (cells only), under white light irradiation (PDT), under 812 nm laser irradiation (PTT), and PDT+PTT, respectively. Cells, 200k/sample; probes, 0.2 nM. *p* values were calculated by Student's *t* -test: *$p < 0.05$, **$p < 0.001$, ***$p < 0.0001$, $n = 3$.

increase the temperature from 25 °C to 55 °C. Even in a wider temperature range than obtained from NIR irradiation, ASP-T_{32} still showed a lower percent fluorescence enhancement than ASP-T_{32} linked to NRs. These results can be attributed to the release of Ce6 from the gold surface, leading to fluorescence recovery and resulting in a higher SOSG signal.

Figure 8 shows the combined PDT/PTT therapy data, expressed as the mean ± standard deviation. The statistical differences were assessed by Student's *t*-test. The control cells, which were incubated with AuNRs-ASP-Ce6, but without any light irradiation, showed no damage (Figure S4 in the Supporting Information). After white light irradiation of CCRF-CEM cancer cells, the cell viability decreased to about 80% ($p < 0.05$) because the photosensitizer was excited by white light,[19,35] leading to the photodynamic killing of cancer cells. To demonstrate the multimodal effect of AuNR-ASP-Ce6 conjugates, NIR laser (812 nm) irradiation for 10 min decreased the cell viability of CCRF-CEM cancer cells to 63% ($p < 0.05$) based on the photothermal killing of cancer cells. However, by using AuNRs-ASP-Ce6 conjugates as agents for both PDT and PTT, the cell viability was just under 40% ($p < 0.0001$), indicating that AuNRs-ASP-Ce6 conjugates can destroy cancer cells more efficiently when used for both PDT and PTT. In contrast, PDT/PTT cytotoxicity to nontarget Ramos (Figure S1) cells was negligible, with cell viability of about 88%.

CONCLUSIONS

In summary, Ce6-ASP-NR composites have been successfully designed for multimodal cancer therapy. The ASP undergoes a structural change in the presence of target cancer cells to drive Ce6 away from the gold surface, thereby producing singlet oxygen for PDT upon light irradiation. However, AuNRs, which can convert light to heat, can also destroy cells by a hyperthermia effect to produce a unique photothermal therapy modality. Combined with the high selectivity and specificity of ASP, this PDT/PTT multimodal strategy promises to be a more efficient therapeutic regimen against cancer cells than either PDT or PTT alone.

MATERIALS AND METHODS

Preparation of AuNRs. AuNRs were prepared according to the seed-mediated protocol using CTAB as a soft template.[31] First, in the presence of 7.5×10^{-2} M CTAB solution, gold seeds were prepared by reducing 2.5×10^{-4} M $HAuCl_4 \cdot 4H_2O$ with 9.0 × 10^{-4} M ice-cold $NaBH_4$. During vigorous stirring, the mixture rapidly developed a light brown color; the solution was then kept at 25 °C before further use. A 25.0 mL growth solution was prepared containing $HAuCl_4 \cdot 4H_2O$ (4.0×10^{-4} M) and CTAB (9.5×10^{-2} M), followed by the addition of 0.15 mL of 0.01 M

$AgNO_3$ and 0.16 mL of 0.1 M L-ascorbic acid (L-AA). During mixing, the solution immediately became colorless. Finally, 0.11 mL of 2 h-aged gold seed solution was added to the above solution and stirred vigorously for 20 s, with the color gradually becoming red. The mixed solution was left undisturbed overnight for further growth.

DNA Synthesis. All DNA oligomers (sequences in Table S1 in the Supporting Information) were synthesized in our lab with an ABI3400 DNA/RNA synthesizer (Applied Biosystems, Foster City, CA, USA). DNA oligomers were deprotected in AMA (ammonium hydroxide/40% aqueous methylamine, 1:1) solution at 65 °C for 20−30 min and then transferred to 15 mL plastic tubes and mixed with 250 μL of 3.0 M NaCl and 6.0 mL of ethanol, followed by placement into a −20 °C freezer for precipitation. After centrifugation at 4000 rpm at 4 °C for 15−30 min, the precipitated DNA products were dissolved in 400 μL of 0.2 M trithylamine acetate (Glen Research Corp.) for HPLC purification with a C-18 reverse-phase HPLC column (ProStar, Varian, Walnut Creek, CA, USA). The collected DNA products were dried and detritylated by dissolving in 200 μL of 80% acetic acid for 20 min at room temperature and then precipitated with 20 μL of 3.0 M NaCl and 500 μL of ethanol at −20 °C, followed by drying with a vacuum dryer. Finally, the concentrations of DNA oligomers were measured with a Cary Bio-300 UV spectrometer (Varian, Walnut Creek, CA, USA).

Synthesis of Aptamer−Photosensitizer. The aptamer−photosensitizer conjugate synthesis includes the on-machine synthesis and the off-machine coupling of chlorine e6 (Frontier Scientific, Inc.). The DNA synthesis on-machine was carried out on the ABI 3400 DNA synthesizer, as described in the DNA Synthesis section. To couple Ce6, which contains three carboxyl groups, we used 3′-amino controlled pore glass (CPG) as a DNA functional group. After finishing DNA synthesis, the fmoc protective group of 3′-amino CPG was removed by 15% 1,5-diazabicyclo-(5.4.0)undec-5-ene. To improve the coupling efficiency, the concentration of Ce6 was 10 times greater than the concentration of the DNA product in the coupling reaction. In 500 μL of *N*, *N*-dimethylformamide (Sigma-Aldrich Inc.), 10 μmol of Ce6 was mixed with an equal molecular amount of *N*,*N*′-dicyclohexylcarbodiimide (Sigma-Aldrich Inc.) and *N*-hydroxysuccinimide (Sigma-Aldrich Inc.). After the activation reaction with 24 h stirring, the sample was washed with acetonitrile until clear and then dried by a vacuum dryer. After deprotection with AMA, aptamer−photosensitizer was further purified by reverse-phase HPLC. Finally, the concentration was measured by a Varian Cary Bio-300 UV spectrometer.

Functionalization of AuNRs with Thiol-Modified Probe. The functionalization of AuNRs followed a published protocol in our laboratory.[7] Before conjugation, the thiol-functionalized oligomers (0.1 mM) were activated by 0.l mM TCEP in 50 mM PBS (pH 7.4) buffer for 1 h at room temperature. To decrease the excess CTAB, the as-prepared AuNR solution (10.0 mL) was centrifugated at 14000 rpm for 10 min, and the precipitate was redispersed with water. To stabilize and functionalize, 10.0 mL of Au NRs were coated with 200 μL of freshly prepared mPEG-SH (2.0 mM). The resultant mixture sat for 1 h at room temperature, followed by the addition of deprotected thiol-aptamer. The mixtures were then incubated for 16 h, aged for another 12 h with 0.2 M NaCl, and finally purified by centrifugation at 12 000 rpm for 5 min.

Evaluation of SOG. All fluorescence measurements were performed using a Fluorolog-3 spectrofluorometer (Jobin Yvon Horiba). A 120 μL microcuvette was used for the spectrofluorometer experiments. To evaluate the SOG of probe samples, the SOSG was introduced at a concentration of 2.0 μM using 50% D_2O as solvent. The SOSG fluorescence was read with the excitation at 494 nm and the maximum emission at 534 nm after the irradiation. For evaluating SOG induced by cDNA, a 10-fold greater concentration of cDNA than ASP-T_{32} was added and incubated at 37 °C for 0.5 h.

Cell Culture. CCRF-CEM (CCL-119, T-cell line, human ALL) and Ramos (CRL-1596, B-cell line, human Burkitt's lymphoma) were cultured in RPMI 1640 medium (Amezrican Type Culture Collection) with 10% fetal bovine serum (FBS, Invitrogen, Carlsbad, CA, USA) and 0.5 mg/mL penicillin−streptomycin (American Type Culture Collection) at 37 °C under a 5% CO_2 atmosphere. Cells were washed before and after incubation with washing buffer [4.5 g/L glucose and 5 mM $MgCl_2$ in Dulbecco's PBS with calcium chloride and magnesium chloride (Sigma-Aldrich)]. Binding buffer used for selection was prepared by adding yeast tRNA (0.1 mg/mL; Sigma-Aldrich) and BSA (1 mg/mL; Fisher Scientific) to the wash buffer to reduce background binding.

Flow Cytometric Analysis. In flow cytometry tubes, 200 nM aptamer, or aptamer on nanorod equivalent, was incubated with 200k CCRF-CEM or Ramos cells at 4 or 37 °C for 2 h in 200 μL of binding buffer. The cells were washed twice with 1 mL of washing buffer, centrifuged at 1260 rpm for 3 min, then resuspended in 100 μL of binding buffer and analyzed on a FacsScan flow cytometer (channel #1 for FAM).

Trypsin Treatment of Cells. First, cells were incubated with aptamer or random sequence at 4 or 37 °C for 2 h. They were then washed with 1 mL of washing buffer to remove the unbound DNA sequences and FBS in the medium or the binding buffer to avoid interference with the function of trypsin, then incubated with trypsin (500 μL, 0.05%)/EDTA (0.53 mm) in HBSS at 37 °C for 10 min. After the incubation, the cells were washed twice with 1 mL of washing buffer and suspended in binding buffer (100 μL with 0.1% NaN_3) for the flow cytometric analysis.

Study of Temperature Enhancement in Cells Bound with AuNR. It is reported that AuNRs are good hyperthermia agents,[1,3] as they are able to induce a temperature increase when they absorb NIR radiation.[36] AuNRs were incubated with cells at 37 °C for 2 h and centrifuged at 1260 rpm for 3 min to remove the unbound NRs. The temperature curve was recorded in real time with a Quarto-FAP System.

Cytotoxicity Study. The cytotoxicity study was performed using the CellTiter 96 Aqueous One Solution cell proliferation assay (MTS) for CCRF-CEM and Ramos cell lines in a 96-well cell culture plate at 200k/well. First, the cells were allowed to bind with NRs-ASP conjugates for 2 h at 37 °C, followed by centrifugation at 1260 rpm for 3 min to remove the unbound NRs-ASP. Cells were then irradiated with laser or white light and then incubated at 37 °C under 5% CO_2 for 48 h, during which cells grew in log phase. Finally, a six-times-diluted MTS solution (120 μL/well) in PRMI-1640 medium solution was added to each well and incubated at 37 °C for 2 h. The absorbance value at 490 nm was determined by a VersaMax microplate reader (Molecular Devices, Inc.).

Conflict of Interest: The authors declare no competing financial interest.

Acknowledgment. We thank Dr. Kathryn R. Williams for editing the manuscript and John W. Munson for detecting the temperature curve with a laser sensor. J.W. received financial support from the China Scholarship Council (CSC). We acknowledge funding through U.S. NIH grants, the China NSFC (20805038, 21035005), and the National Basic Research Program of China (2007CB935603, 2010CB732402), as well as the China National Grand Program on Key Infectious Disease (2009ZX10004-312) for partial support.

Supporting Information Available: Additional information as noted in the text. This material is available free of charge *via* the Internet at http://pubs.acs.org.

REFERENCES AND NOTES

1. Kuo, W.-S.; Chang, C.-N.; Chang, Y.-T.; Yang, M.-H.; Chien, Y.-H.; Chen, S.-J.; Yeh, C.-S. Gold Nanorods in Photodynamic Therapy, as Hyperthermia Agents, and in Near-Infrared Optical Imaging. *Angew. Chem., Int. Ed.* **2010**, *49*, 2711–2715.
2. Kah, J. C. Y.; Wan, R. C. Y.; Wong, K. Y.; Mhaisalkar, S.; Sheppard, C. J. R.; Olivo, M. Combinatorial Treatment of Photothermal Therapy Using Gold Nanoshells with Conventional Photodynamic Therapy to Improve Treatment Efficacy: An *In Vitro* Study. *Laser Surg. Med.* **2008**, *40*, 584–589.
3. Jang, B.; Park, J.-Y.; Tung, C.-H.; Kim, I.-H.; Choi, Y. Gold Nanorod-Photosensitizer Complex for Near-Infrared

Fluorescence Imaging and Photodynamic/Photothermal Therapy *in Vivo*. *ACS Nano* **2011**, *5*, 1086–1094.
4. Barth, B. M.; Altnoğlu, E. I.; Shanmugavelandy, S. S.; Kaiser, J. M.; Crespo-Gonzalez, D.; DiVittore, N. A.; McGovern, C.; Goff, T. M.; Keasey, N. R.; Adair, J. H.; *et al*. Targeted Indocyanine-Green-Loaded Calcium Phosphosilicate Nanoparticles for *in Vivo* Photodynamic Therapy of Leukemia. *ACS Nano* **2011**, *26*, 5325–5337.
5. Oseroff, A. R.; Ohuoha, D.; Hasan, T.; Bommer, J. C.; Yarmush, M. L. Antibody-Targeted Photolysis: Selective Photodestruction of Human T-Cell Leukemia Cells Using Monoclonal Antibody-Chlorin e6 Conjugates. *Proc. Natl. Acad. Sci. U. S. A.* **1986**, *83*, 8744–8748.
6. Huang, Y.-F.; Sefah, K.; Bamrungsap, S.; Chang, H.-T.; Tan, W. Selective Photothermal Therapy for Mixed Cancer Cells Using Aptamer-Conjugated Nanorods. *Langmuir* **2008**, *24*, 11860–11865.
7. Huang, Y.-F.; Chang, H.-T.; Tan, W. Cancer Cell Targeting Using Multiple Aptamers Conjugated on Nanorods. *Anal. Chem.* **2008**, *80*, 567–572.
8. Koo, H.; Huh, M. S.; Sun, I.-C.; Yuk, S. H.; Choi, K.; Kim, K.; Kwon, I. C. *In Vivo* Targeted Delivery of Nanoparticles for Theranosis. *Acc. Chem. Res.* **2011**, *44*, 1018–1028.
9. Wang, H.; Yang, R.; Yang, L.; Tan, W. Nucleic Acid Conjugated Nanomaterials for Enhanced Molecular Recognition. *ACS Nano* **2009**, *3*, 2451–2460.
10. Kong, R.-M.; Zhang, X.-B.; Chen, Z.; Tan, W. Aptamer-Assembled Nanomaterials for Biosensing and Biomedical Applications. *Small* **2011**, *7*, 2428–2436.
11. Wang, J.; Zhang, P.; Li, J. Y.; Chen, L. Q.; Huang, C. Z.; Li, Y. F. Adenosine-Aptamer Recognition-Induced Assembly of Gold Nanorods and a Highly Sensitive Plasmon Resonance Coupling Assay of Adenosine in the Brain of Model SD Rat. *Analyst* **2010**, *135*, 2826–2831.
12. Song, S.; Wang, L.; Li, J.; Zhao, J.; Fan, C. Aptamer-Based Biosensors. *Trends Anal. Chem.* **2008**, *27*, 108–117.
13. Zhen, S. J.; Chen, L. Q.; Xiao, S. J.; Li, Y. F.; Hu, P. P.; Zhan, L.; Peng, L.; Song, E. Q.; Huang, C. Z. Carbon Nanotubes as a Low Background Signal Platform for a Molecular Aptamer Beacon on the Basis of Long-Range Resonance Energy Transfer. *Anal. Chem.* **2010**, *82*, 8432–8437.
14. Fang, X.; Tan, W. Aptamers Generated from Cell-SELEX for Molecular Medicine: A Chemical Biology Approach. *Acc. Chem. Res.* **2010**, *43*, 48–57.
15. Tang, Z.; Shangguan, D.; Wang, K.; Shi, H.; Sefah, K.; Mallikratchy, P.; Chen, H. W.; Li, Y.; Tan, W. Selection of Aptamers for Molecular Recognition and Characterization of Cancer Cells. *Anal. Chem.* **2007**, *79*, 4900–4907.
16. Sefah, K.; Tang, Z.; Shangguan, D.; Chen, H.; Lopez-Colon, D.; Li, Y.; Parekh, P.; Martin, J.; Meng, L.; Phillips, J. A.; *et al*. Molecular Recognition of Acute Myeloid Leukemia Using Aptamers. *Leukemia* **2009**, *23*, 235–244.
17. Chen, X.; Huang, Y.; Tan, W. Using Aptamer-Nanoparticle Conjugates for Cancer Cells Detection. *J. Biomed. Nanotechnol.* **2008**, *4*, 400–409.
18. Tan, W.; Wang, H.; Chen, Y.; Zhang, X.; Zhu, H.; Yang, C.; Yang, R.; Liu, C. Molecular Aptamers for Drug Delivery. *Trends Biotechnol.* **2011**, *29*, 634–640.
19. Wang, K.; You, M.; Chen, Y.; Han, D.; Zhu, Z.; Huang, J.; Williams, K.; Yang, C. J.; Tan, W. Self-Assembly of a Bifunctional DNA Carrier for Drug Delivery. *Angew. Chem., Int. Ed.* **2011**, *50*, 6098–6101.
20. Wu, Z.; Tang, L.-J.; Zhang, X.-B.; Jiang, J.-H.; Tan, W. Aptamer-Modified Nanodrug Delivery Systems. *ACS Nano* **2011**, *5*, 7696–7699.
21. Chang, M.; Yang, C.-S.; Huang, D.-M. Aptamer-Conjugated DNA Icosahedral Nanoparticles As a Carrier of Doxorubicin for Cancer Therapy. *ACS Nano* **2011**, *5*, 6156–6163.
22. Kim, D.; Jeong, Y. Y.; Jon, S. A Drug-Loaded Aptamer-Gold Nanoparticle Bioconjugate for Combined CT Imaging and Therapy of Prostate Cancer. *ACS Nano* **2010**, *4*, 3689–3696.
23. Tang, Z.; Zhu, Z.; Mallikaratchy, P.; Yang, R.; Sefah, K.; Tan, W. Aptamer-Target Binding Triggered Molecular Mediation of Singlet Oxygen Generation. *Chem. Asian J.* **2010**, *5*, 783–786.
24. Shieh, Y.-A.; Yang, S.-J.; Wei, M.-F.; Shieh, M.-J. Aptamer-Based Tumor-Targeted Drug Delivery for Photodynamic Therapy. *ACS Nano* **2010**, *4*, 1433–1442.
25. Barth, B. M.; I. Altinoğlu, E.; Shanmugavelandy, S. S.; Kaiser, J. M.; Crespo-Gonzalez, D.; DiVittore, N. A.; McGovern, C.; Goff, T. M.; Keasey, N. R.; Adair, J. H.; *et al*. Targeted Indocyanine-Green-Loaded Calcium Phosphosilicate Nanoparticles for *in Vivo* Photodynamic Therapy of Leukemia. *ACS Nano* **2011**, *5*, 5325–5337.
26. Chari, R. V. J. Targeted Cancer Therapy: Conferring Specificity to Cytotoxic Drugs. *Acc. Chem. Res.* **2008**, *41*, 98–107.
27. Chin, W. W. L.; Heng, P. W. S.; Olivo, M. Chlorin e6-Polyvinylpyrrolidone Mediated Photosensitization is Effective Against Human Non-Small Cell Lung Carcinoma Compared to Small Cell Lung Carcinoma Xenografts. *BMC Pharm.* **2007**, *7*, 15.
28. Shi, H.; He, X.; Wang, K.; Wu, X.; Ye, X.; Guo, Q.; Tan, W.; Qing, Z.; Yang, X.; Zhou, B. Activatable Aptamer Probe for Contrast-Enhanced *in Vivo* Cancer Imaging Based on Cell Membrane Protein-Triggered Conformation Alteration. *Proc. Natl. Acad. Sci. U. S. A.* **2011**, *108*, 3900–3905.
29. Tang, Z.; Mallikaratchy, P.; Yang, R.; Kim, Y.; Zhu, Z.; Wang, H.; Tan, W. Aptamer Switch Probe Based on Intramolecular Displacement. *J. Am. Chem. Soc.* **2008**, *130*, 11268–11269.
30. Alkilany, A. M.; Thompson, L. B.; Boulos, S. P.; Sisco, P. N.; Murphy, C. J. Gold Nanorods: Their Potential for Photothermal Therapeutics and Drug Delivery, Tempered by the Complexity of Their Biological Interactions. *Adv. Drug Delivery Rev.* **2012**, *64*, 190–199.
31. Wang, J.; Li, Y. F.; Huang, C. Z. Identification of Iodine-Induced Morphological Transformation of Gold Nanorods. *J. Phys. Chem. C* **2008**, *112*, 11691–11695.
32. Huang, P.; Li, Z.; Lin, J.; Yang, D.; Gao, G.; Xu, C.; Bao, L.; Zhang, C.; Wang, K.; Song, H.; *et al*. Photosensitizer-Conjugated Magnetic Nanoparticles for *in Vivo* Vimultaneous Magnetofluorescent Imaging and Targeting Therapy. *Biomaterials* **2011**, *32*, 3447–3458.
33. Shangguan, D.; Li, Y.; Tang, Z.; Cao, Z. C.; Chen, H. W.; Mallikaratchy, P.; Sefah, K.; Yang, C. J.; Tan, W. Aptamers Evolved from Live Cells as Effective Molecular Probes for Cancer Study. *Proc. Natl. Acad. Sci. U. S. A.* **2006**, *103*, 11838–11843.
34. Xiao, Z.; Shangguan, D.; Cao, Z.; Fang, X.; Tan, W. Cell-Specific Internalization Study of an Aptamer from Whole Cell Selection. *Chem.—Eur. J.* **2008**, *14*, 1769–1775.
35. Zhu, Z.; Tang, Z.; Phillips, J. A.; Yang, R.; Wang, H.; Tan, W. Regulation of Singlet Oxygen Generation Using Single-Walled Carbon Nanotubes. *J. Am. Chem. Soc.* **2008**, *130*, 10856–10857.
36. Jang, B.; Kim, Y. S.; Choi, Y. Effects of Gold Nanorod Concentration on the Depth-Related Temperature Increase during Hyperthermic Ablation. *Small* **2010**, *7*, 265–270.
37. Luo, Y.-L.; Shiao, Y.-S.; Huang, Y.-F. Release of Photoactivatable Drugs from Plasmonic Nanoparticles for Targeted Cancer Therapy. *ACS Nano* **2011**, *5*, 7796–7804.